NASA TECHNICAL NOTE

NASA TN D-7348

NASA TN D-7348

PROTON-RADIATION DAMAGE IN GUNN OSCILLATORS

by James W. Johnson and Carl L. Fales

Langley Research Center

Hampton, Va. 23665

NATIONAL AERONAUTICS AND SPACE ADMINISTRATION • WASHINGTON, D. C. • DECEMBER 1973

1. Report No.	2. Government Accession No.	3. Recipient's Catalog No.
NASA TN D-7348		

4. Title and Subtitle	5. Report Date
PROTON-RADIATION DAMAGE IN GUNN OSCILLATORS	December 1973
	6. Performing Organization Code

7. Author(s)	8. Performing Organization Report No.
James W. Johnson and Carl L. Fales	L-9042
	10. Work Unit No. 160-20-54-05
9. Performing Organization Name and Address NASA Langley Research Center Hampton, Va. 23665	11. Contract or Grant No.
	13. Type of Report and Period Covered Technical Note
12. Sponsoring Agency Name and Address National Aeronautics and Space Administration Washington, D.C. 20546	14. Sponsoring Agency Code

15. Supplementary Notes

16. Abstract

The irradiation effects of 22 MeV protons on the electrical characteristics of GaAs continuous-wave Gunn oscillators have been studied. The radio-frequency power output was reduced by 3 decibels at proton fluences in the neighborhood of 1.5×10^{12} protons-cm^{-2}. Conductance measurements indicate that the carrier removal rate at high electric fields remained roughly 40 percent less than at low fields. Diode efficiencies of two device groups ($nl \approx 2 \times 10^{12}$ cm^{-2} and $nl \approx 4 \times 10^{12}$ cm^{-2}) were found to be monotonically decreasing functions of fluence, where nl is defined as the density-length product. Frequency-modulation noise was generally unaffected by radiation, but the magnitude of the noise in the noise power spectrum increased significantly. These effects are partially accounted for, in a qualitative fashion, by a model of electron traps having field-dependent net-carrier capture rates and various response times.

17. Key Words (Suggested by Author(s))	18. Distribution Statement
Gunn oscillators Proton-radiation damage	Unclassified – Unlimited

19. Security Classif. (of this report)	20. Security Classif. (of this page)	21. No. of Pages	22. Price*
Unclassified	Unclassified	30 ~~25~~	Domestic, $3.00 Foreign, $5.50

*For sale by the National Technical Information Service, Springfield, Virginia 22151

PROTON-RADIATION DAMAGE IN GUNN OSCILLATORS

By James W. Johnson and Carl L. Fales
Langley Research Center

SUMMARY

The irradiation effects of 22 MeV protons on the electrical characteristics of GaAs continuous-wave Gunn oscillators have been studied. The radio-frequency power output was reduced by 3 decibels at proton fluences in the neighborhood of 1.5×10^{12} protons-cm^{-2}. Conductance measurements indicate that the carrier removal rate at high electric fields remained roughly 40 percent less than at low fields. Diode efficiencies of two device groups $\left(n\ell \approx 2 \times 10^{12}\ cm^{-2}\right.$ and $\left.n\ell \approx 4 \times 10^{12}\ cm^{-2}\right)$ were found to be monotonically decreasing functions of fluence, where $n\ell$ is defined as the density-length product. Frequency-modulation noise was generally unaffected by radiation, but the magnitude of the noise in the noise power spectrum increased significantly. These effects are partially accounted for, in a qualitative fashion, by a model of electron traps having field-dependent net-carrier capture rates and various response times.

INTRODUCTION

Except for nuclear transmutations, the semipermanent damage induced by radiation in the bulk of a semiconductor is in the form of lattice defects caused by the displacement of atoms within the crystal. These defects are comprised of interstitial atoms, their vacated sites (vacancies), and various interacting complexes such as di-vacancies and vacancy-impurity atom combinations. The creation of lattice defects has electrical consequences by the introduction of scattering centers and of energy levels into the forbidden gap which behave as donors, acceptors, or recombination centers. The type and energy of the bombarding particles play an important role in the damage process. In space applications, the typical particles are electrons and protons (in the Van Allen belts and solar flare incidents) and neutrons and gamma rays (from RTG aboard spacecraft).

Pertinent to the present discussion are a number of radiation studies on GaAs: reference 1 for proton effects on solar cells, references 2 to 6 for fast neutrons, and references 2, 3, and 7 for electrons or gamma rays. References 4, 6, and 7 discuss gamma and neutron radiation effects on GaAs Gunn diodes. The conclusions drawn from these studies are similar to the general comments previously mentioned. The carrier concentration and low field mobility are found to be important radiation-sensitive n-type

GaAs properties basic to Gunn oscillator performance. Slow electron traps (time constant ≈ 3 msec) introduced by fast neutron irradiation have been observed in Gunn diodes (ref. 6). The model of reference 6 explaining this effect assumes that the trap capture rate increases when the electric field exceeds threshold and gives a reduced carrier density in continuous wave (cw) operation.

In the present investigation, the results of dc and rf measurements made on GaAs cw Gunn oscillators after 22 MeV proton bombardments are reported. Presented are analyses suggesting that the carrier density is significantly greater at high fields than at low fields, the difference increasing with proton exposures. For example, the electron traps introduced by the irradiations have net-capture rates that are smaller at high fields than at low fields. Changes in carrier mobility are considered small relative to those of carrier density. Power output and efficiency degradations are attributed to reductions in carrier density and peak-to-valley current ratio and to production of traps whose response times are intermediate to those termed fast and slow. Frequency-modulation noise is generally unaffected by radiation, and changes in frequency drift are relatively small. In contrast, the magnitude of the noise in the noise power spectrum increases significantly.

SYMBOLS

A	cross-sectional area of active device region
$C(\bar{n})$	Copeland curve
c	capture rate per center
D_1, D_2	diodes having $nl \approx 2 \times 10^{12}$ cm^{-2}
D_3, D_4, D_5	diodes having $nl \approx 4 \times 10^{12}$ cm^{-2}
E	electron energy
E_{a_i}	radiation induced acceptor energy
E_D	chemical donor concentration
E_{d_i}	radiation induced donor energy
E_f	Fermi energy

e	electron charge
G	low-field conductance
G_o	preirradiation low-field conductance
g	generation rate
I	device direct current
I_v	valley current
I_{v_o}	preirradiation valley current
$I_p)_{os}$	peak current under oscillating conditions
$I_v)_{os}$	valley current under oscillating conditions
J_e	particle current
l	length of active device region
N	density of occupied traps
N_{a_i}	radiation-induced acceptor concentrations
N_D	chemical donor concentration
N_{d_i}	radiation-induced donor concentrations
N_t	density of traps
n	low-field electron density
n_o	preirradiation electron density
$\tilde{n}$	electron density under oscillating conditions
n'	high-field electron density

n'_o	preirradiation high-field electron density
n^+-n-n^+	doping profile of Gunn diodes used
$\left.\frac{\partial n}{\partial t}\right)_{tr}$	net generation rate from traps
r	dynamic peak-to-valley current ratio
$\bar{r}$	direct-current peak-to-valley current ratio
t	time
V	device direct-current voltage
V_T	diode threshold voltage
$v(\epsilon)$	field-dependent drift velocity
v_s	saturation or scattering-limited drift velocity
x	lineal distance through semiconductor
α	carrier removal rate
α'	field dependent carrier removal rate
α_{a_i}	acceptor production rate
α_{d_i}	donor production rate
ϵ	electric field
ϵ_T	threshold electric field
κT	Boltzmann constant × absolute temperature
μ	low-field carrier mobility

τ trap response time

Φ proton fluence

EXPERIMENTAL PROCEDURES

The devices under test were irradiated with 22 MeV protons at the Oak Ridge National Laboratory's 86-inch (2.18 m) cyclotron. The proton beam uniformity was improved by passing the beam through a scattering foil and a 1-inch (2.54 cm) diameter collimator. The beam current was monitored with a specially designed thin window ion chamber which had been calibrated with a Faraday cup. A current integrator monitored the ion chamber current and gave a direct measure of proton fluence. The proton flux rate for the experiment was about 10^9 protons-cm^{-2}-sec^{-1}. Each device was irradiated through its 0.53 mm brass contact and oriented such that the beam was normal to the semiconductor chip.

Five Varian Associates VSX-9201 X-band diodes with nominal initial electron densities n_o of 2.2×10^{15} cm^{-3} $(D_1$ and $D_2)$ and 4.0×10^{15} cm^{-3} $(D_3$, D_4, and $D_5)$ and active region thicknesses of 10 μm and 11 μm, respectively, were used. All devices had n^+-n-n^+ sandwich structures. Four of these were each exposed to a maximum fluence Φ of 3.0×10^{12} protons-cm^{-2} in as many as seven increments; and one diode (D_1) failed before reaching this level. A Varian VSX-9001 waveguide cavity was used with the tuning probe adjusted for a nominal operating frequency of 9 GHz. This adjustment was left unchanged and cavity temperature remained near ambient throughout the tests. The following electrical measurements were made on all five diodes:

(a) Current-voltage characteristics

(b) Output power and frequency into a matched termination as a function of bias voltage

(c) Maximum output power (optimum load) and frequency as a function of bias voltage

(d) FM noise spectrum in the band from 100 hertz to 50 kilohertz

(e) Frequency drift over a 10-minute period

(f) Noise power spectrum out to 1 MHz from the carrier

The radio-frequency measurement system is shown in figure 1. Low-field conductance was calculated by using current-voltage curves which were generated with the diodes mounted in the cavity. When the contact series resistance was assumed to remain small under irradiation, this method was sufficient to resolve conductance (carrier concentra-

tion) as a function of fluence. Maximum output power was measured at 9 volts bias with oscillator loading optimized by the E-H tuner. Efficiency was calculated from the maximum output power at 9 volts. A Hewlett Packard 2590-A microwave frequency converter made it possible to monitor the frequency drift of the X-band signal. Frequency-modulation noise properties were determined with the same Hewlett Packard 2590-A used as a frequency-modulation detector and a General Radio 1900-A/1521-B wave analyzer/recorder. A 10-Hz bandwidth was selected on the wave analyzer, and the data were corrected by a factor of 10 to give the corresponding noise in a 1000-Hz bandwidth. A phase-locked klystron functioning as a local oscillator and a Hewlett Packard 312-A wave analyzer were the fundamental components in the noise power-spectrum measurements. A filter bandwidth of 3000 Hz was used on the 312-A analyzer. Thus, the noise power spectrum is discussed herein in terms of the ratio of signal power to the noise power in a 3000-Hz bandwidth centered about a given point with respect to the signal.

Each diode was removed from the mount, irradiated, and replaced. There was no significant change in oscillator performance as a result of removing and reinserting the diode.

RESULTS

Power and Efficiency

A typical set of current-voltage curves for various proton-fluence levels is shown in figure 2. Note the decrease in low-field conductance, saturation (valley) current, and the peak-to-valley current ratio. The threshold voltage for the negative differential resistivity region is relatively insensitive to the radiation levels attained in this experiment. The low-field conductance, saturation current, and peak-to-valley current ratio are plotted as a function of proton fluence in figures 3, 4, and 5, respectively. Diodes D_3, D_4, and D_5 appear to behave in a similar fashion in the experiment, as might be expected for devices fabricated from the same semiconductor chip. These effects manifest themselves as a degradation in output power and efficiency, although the relationship of dc peak-to-valley current ratio to efficiency must be carefully qualified. (See subsequent section on "Efficiency.") Maximum output power as a function of fluence is shown in figure 6. All of the devices had degraded by 3 decibels or more at a fluence of 1.5×10^{12} protons-cm^{-2}. At approximately 2.0×10^{12} protons-cm^{-2}, D_1 had failed, and a fluence of 3.0×10^{12} protons-cm^{-2} caused at least a 10-decibel drop in power for diodes D_2 to D_5. Merely sustaining oscillations became critically dependent upon loading and bias voltage; thus, all five diodes had essentially failed at this fluence level. Prior to failure, the changing impedances of the devices resulted in frequency shifts of 0.25 percent operating into a matched termination. Figure 7 shows efficiency as a function of fluence. The significant feature in these curves is that efficiency for diodes D_3

to D_5 is a monotonically decreasing function of fluence as found by Marcus and Bruemmer (ref. 4) rather than peaking as observed by Brehm (ref. 7) and Stein (ref. 3) with gamma, electron, and neutron irradiation.

Noise

Recent FM noise tests with gamma radiation (ref. 7) showed no significant increase in diode noise in the 100-Hz to 50-kHz band. Likewise with proton radiation, four out of the five diodes tested (D_1, D_2, D_3, and D_5) exhibited no additional noise in this same band up to the point of device failure. The FM noise properties of diode D_4 did change as shown in figure 8. The dashed line is the noise threshold of the measurement system; however, the preirradiation curve can be extrapolated at a rate of 6 dB/octave from 10 kHz to 50 kHz (ref. 8). Below 20 kHz, the root-mean-square deviation of diode D_4 increased by as much as 6 dB; and the change was even greater between 20 kHz and 50 kHz where the curve began to rise. There is no apparent explanation for the anomalous behavior of this particular diode.

Peak-to-peak frequency drift increased by factors that ranged from slightly greater than 1.0 to 3.5. Figure 9 shows the results from diode D_1 where the drift increased by approximately a factor of 2.0. These changes are relatively small in light of the fact that at this point the devices were on the verge of complete failure (essentially zero output power).

The change in the positive and negative halves of the noise power spectrum of diode D_3 after a fluence of 3.0×10^{12} protons-cm^{-2} is shown in figure 10. The signal-to-noise ratio that describes the spectrum increased by approximately 14 dB across the measurement band, which was typical of all five devices.

DISCUSSION

Carrier Removal Effects

The current-voltage curves are essentially flat beyond 10 volts and up to 20 volts $\left(\frac{V}{l} \approx 20 \text{ kV/cm}\right)$ where there is negligible rf signal from the devices. Thus, the measurement of valley current at $V = 10$ volts adequately represents the case where the electric field exceeds threshold through most of the active GaAs region. Further, the nature of the n^+-n-n^+ sandwich structure is such that the magnitude of any anomalously high electric fields in the cathode region are kept to a minimum. It is assumed in this study that scattering-limited velocities are attained throughout the active device region for high enough applied voltages. This assumption in turn implies a uniform carrier density under these conditions.

The electron traps introduced by the proton irradiations may fall into any or all of three groups according to their response times, τ:

Fast traps, $\tau \ll$ Gunn oscillation period $\approx 10^{-10}$ sec

Slow traps, $\tau \gg 10^{-10}$ sec

Intermediate, $\tau \approx 10^{-10}$ sec

Therefore, the dc valley current, I_V, reflects a situation where all traps, whether fast or slow, are effective in the removal of electrons from the conduction band. It is then desirable to investigate the electric field dependence of these traps, that is, low field relative to high field.

A central assumption made is that, approximately, at low fields,

$$I = \frac{n\mu eAV}{l} \tag{1}$$

and at high fields

$$I_V = n' v_S eA \tag{2}$$

The drift velocity v_S is considered to be relatively independent of proton fluence for the radiation exposure levels encountered. Thus, even in cases where the low-field mobility is being degraded, the scattering effectiveness of charged defect centers becomes smaller for increasing (nonrelativistic) carrier velocities or high electric fields; and the carrier velocity remains mostly phonon scattering limited. Using typical preirradiation values for $v_S (\approx 10^7$ cm/sec) and $\mu (\approx 7.5 \times 10^3$ cm^2/V-sec) and the nominal carrier densities for devices D_1 to D_5, one obtains from equations (1) and (2) good agreement between the measured and calculated values of I and I_V by assuming that $n = n'$. If it is supposed that $n = n'$ for all values of Φ, then, from equations (1) and (2) it should be possible to relate changes in n and μ with respect to fluence to the measurements of low-field conductance and valley current. Hence, $n/n_0 = I_V/I_{V_0}$ and $\mu/\mu_0 = (G/G_0)(n/n_0)^{-1}$, where $G = \frac{I}{V}$ in the low-field region. However, when these relations are assumed, with proton irradiation, changes in mobility as a function of fluence are found to occur at about the same rate as changes in carrier concentration. This result is not acceptable because of the following experimental and theoretical observations.

Electron and gamma-ray damage consists of point defects while that of fast neutrons consist primarily of disordered regions. One illustration of this result is found in reference 2 where for a given change in carrier density the change in reciprocal mobility

was 2 to 4 times greater for fast neutrons than for 1 MeV electrons in n-type GaAs. For Gunn quality GaAs, references 3 and 4 (neutrons) and reference 7 (gammas) report only small changes in mobility relative to changes in carrier concentration for irradiations near room temperature. In contrast, reference 6 shows changes in mobility relative to changes in carrier concentration of roughly 25 to 40 percent.

Moderate energy protons (22 MeV) are expected to be intermediate between fast neutrons and electrons in the type of lattice defects produced (ref. 9). Low-energy collisions are more probable with protons because of the coulombic interaction with the lattice nuclei as opposed to the hard sphere collisions by neutrons. It is assumed herein that changes in mobility can be neglected relative to those in carrier concentration. It follows that

$$\left.\begin{aligned} \frac{n}{n_O} &= \frac{G}{G_O} \\ \text{and} \\ \frac{n'}{n_O} &= \frac{I_V}{I_{V_O}} \end{aligned}\right\} \tag{3}$$

where

$$n_O \approx n'_O$$

Several comments are necessary before the experimental results are discussed. For an n-type extrinsic semiconductor that is relatively uncompensated, the electron density is, in thermodynamic equilibrium (low fields),

$$n = N_D\left[1 - f\left(E_d\right)\right] + \sum_i \left[1 - f\left(E_{d_i}\right)\right]N_{d_i} - \sum_i f\left(E_{a_i}\right)N_{a_i} \tag{4}$$

where N_{d_i} and N_{a_i} are the radiation induced donor and acceptor concentrations at E_{d_i} and E_{a_i}, respectively. The chemical donor concentration is N_D, and $f(E)$ is the Fermi distribution

$$f(E) = \left[1 + e^{\left(E-E_f\right)/\kappa T}\right]^{-1} \tag{5}$$

where E_f = Fermi energy. Assume that all pertinent energy levels are at least several κT away from the initial Fermi level. Indeed, for GaAs, in the process of reducing carrier density by radiation from 2×10^{15} cm^{-3} to 1×10^{15} cm^{-3}, the Fermi level changes by $0.693\kappa T$. Thus, all levels remain several κT away from the Fermi energy for all intermediate degrees of carrier removal. If all the rates of introduction of N_{d_i} and N_{a_i} with proton fluence are of the same order of magnitude, then it follows immediately that the fraction of acceptors above E_f that are occupied remains negligible, and the fraction of donors above E_f that are ionized remains near 1. Similarly, the fraction of acceptors below E_f that are occupied remains near 1, and the fraction of donors below E_f that are ionized remains negligible. Thus, in the carrier removal process just discussed,

$$n \approx N_D + \sum_{i\left(E_{d_i} > E_f\right)} N_{d_i} - \sum_{i\left(E_{d_i} < E_f\right)} N_{a_i} \tag{6}$$

For the levels of defect production considered, the concentrations expected are

$$N_{d_i} = \alpha_{d_i} \Phi$$

and

$$N_{a_i} = \alpha_{a_i} \Phi$$

which yields

$$n \approx n_o - \left[\sum_{i\left(E_{a_i} < E_f\right)} \alpha_{a_i} - \sum_{i\left(E_{d_i} > E_f\right)} \alpha_{d_i}\right] \Phi \equiv n_o - \alpha\Phi \tag{7}$$

and

$$\frac{n}{n_o} = 1 - \left(\frac{\alpha}{n_o}\right)\Phi \tag{8}$$

where $\alpha \equiv$ carrier removal rate.

A suggestive argument for the high-field case can be made by using a crude single species trap model. The rate equation in one dimension is

$$\frac{\partial n}{\partial t} = \left(\frac{\partial n}{\partial t}\right)_{tr} - \frac{\partial J_e}{\partial x} \tag{9}$$

where J_e is the particle current density and $\left.\frac{\partial n}{\partial t}\right)_{tr}$ is the net generation rate from the traps. Neglecting the contributions from the valence band yields

$$\left.\frac{\partial n}{\partial t}\right)_{tr} = -cn\left(N_t - N\right) + gN \tag{10}$$

Note that c and g may depend on the electric field. In a spatially uniform and steady-state case (not in the negative differential resistance region),

$$\left.\frac{\partial n}{\partial t}\right)_{tr} = 0 = -cn\left(N_t - N\right) + gN \tag{11}$$

Assume that the traps are neutral when unoccupied (acceptors). Then $n + N$ = total density of electrons, n_o, and consequently

$$\frac{n}{n_o} = \frac{1}{2}\left(1 - \frac{N_t}{n_o} - \frac{g}{cn_o}\right) + \frac{1}{2}\sqrt{\left(1 - \frac{N_t}{n_o} - \frac{g}{cn_o}\right)^2 + 4\,\frac{g}{cn_o}} \tag{12}$$

In the thermodynamic equilibrium (low field) case, equation (11) gives

$$\frac{g}{cn_o} = e^{\left(E_t - E_f\right)/\kappa T} \tag{13}$$

for $n = n_o$. For acceptor levels several κT below E_f, $\frac{g}{cn_o} \ll 1$; and from equation (12) the previous result in equation (8) is obtained.

For high electric fields, $\frac{g}{cn_o}$ is not negligible. Values of $\frac{g}{cn_o} \approx 0.4$ and $0 \leqq \frac{N_t}{n_o} \leqq 0.77$ are typical for devices D_1 and D_3. Thus, the following equations are found to be good approximations (within 3 percent) to equation (12)

$$\frac{n}{n_o} = 1 - \left(1 - \frac{g}{cn_o}\right)\frac{N_t}{n_o} \tag{14}$$

or

$$\frac{n}{n_o} = 1 - \frac{\alpha'}{n_o}\,\Phi \tag{15}$$

where $\alpha' \equiv \alpha\left(1 - \frac{g}{cn_o}\right)$ and α is the same as in equation (8). Note that α' can decrease at high fields if g increases, or c decreases, or both. The mechanisms causing such field dependences are discussed subsequently.

Figure 11 is a plot of the normalized carrier density as functions of proton fluence for diodes D_1 and D_3, which are representative of the two groups of Gunn diodes. Except for one data point, the carrier density decreases linearly with fluence. From equations (8) and (15), it follows that

$$\frac{\text{Slope } D_1}{\text{Slope } D_3} = \frac{n_o(D_3)}{n_o(D_1)} = 1.82$$

The experimental values are 1.67 and 1.73 for the n and n' curves, respectively.

The interesting feature of figure 11 is that carrier removal rates for high fields are less than those for low fields. In fact

$$\alpha(D_1) \approx 730 \text{ carriers-cm}^{-1}\text{-protons}^{-1}$$

$$\alpha'(D_1) \approx 450 \text{ carriers-cm}^{-1}\text{-protons}^{-1}$$

$$\alpha(D_3) \approx 806 \text{ carriers-cm}^{-1}\text{-protons}^{-1}$$

$$\alpha'(D_3) \approx 472 \text{ carriers-cm}^{-1}\text{-protons}^{-1}$$

The removal rates at the high fields are roughly 40 percent less than at low fields for $\frac{g}{cn_o} \approx 0.4$ as stated previously for the single trap model.

The basic interactions that must be considered in a transport problem to obtain an electron distribution function are electron-applied electric field, electron-impurity (defect), electron-phonon, electron-photon, electron-electron, and electron-hole. Several well-known effects (combinations of the above) whose origins rest on the presence of high electric fields are:

(1) The capture rate per trapping center is less in magnitude at high fields than at low fields

(2) Impact ionization of traps

(3) Internal field emission from traps to the conduction band

(4) Schottky emission from traps to the conduction band

(5) Hopping of thermally excited electrons between isolated states

Item (1) corresponds to a smaller c in equation (10) while items (2) to (4) give rise to a larger g.

On the other hand the hopping phenomena, item (5), corresponds to a distinct conduction mechanism. Items (3) to (5) are important high-field charge-transport mechanisms in insulators.

Efficiency

It was previously noted that for the experiment described herein, the efficiency is a monotonically decreasing function of fluence as found by Marcus and Bruemmer (ref. 4) rather than peaking as observed by Brehm and Pearson (ref. 7) and Stein (ref. 3). Brehm and Pearson and Stein use Copeland's (ref. 10) theoretical plot of optimum efficiency as a function of carrier concentration to obtain a qualitative description of optimum power output as a function of carrier removal. Their results were consistent with theory, which predicts that efficiency has a maximum value for $n\ell \approx 1 - 2 \times 10^{12}$ cm^{-2}. Maximum power initially increased with a subsequent decrease for diodes having $n\ell \lesssim 1 - 2 \times 10^{12}$ cm^{-2}; on the other hand, maximum power decreased monotonically for diodes having $n\ell \gtrsim 1 - 2 \times 10^{12}$ cm^{-2}.

Efficiency has been shown to be approximately proportional to $(r - 1)/(r + 1)$, where $r \equiv$ peak-to-valley current ratio (refs. 10 and 11). The conditions under which this relation is true must be carefully stated to interpret properly the limits of its applicability. The dependence of efficiency on r is approximately valid if: (1) the I-V or v-ϵ curve from which r is calculated is an instantaneous function of electric field (ref. 11), and (2) using calculations that include diffusion effects (ref. 10), one has a relatively trap-free, active semiconductor region. Thus, r is described as a dynamic peak-to-valley ratio which may be quite different from the low frequency value $\bar{r}$.

Slow traps.- Slow traps cannot respond to rf signal variations, but their field dependence might adjust in cw operation to that corresponding to the average electric field. Clearly r is not equal to $\bar{r}$. It is expected that r is independent of the average carrier density $\bar{n}$ under oscillating conditions, that is, $I_p)_{os} \propto \bar{n}$ and $I_v)_{os} \propto \bar{n}$. If $v(\epsilon)$, v_s, and V_T change relatively little with fluence, then r should be relatively insensitive to irradiation level. Hence, no efficiency degradation due to the factor $(r - 1)/(r + 1)$ is contemplated. It should be possible to attribute the changes in efficiency to carrier removal based on Copeland's curve. The efficiency for diodes D_3 to D_5 would than be expected to increase initially with fluence. This increase was not observed for the proton irradiations, in agreement with reference 4 for fast neutrons. Thus, the possibility of faster traps will be considered in the next section.

Berg and Dropkin (ref. 6) found slow traps ($\tau \approx 3$ μsec) in neutron-irradiated diodes ($n\ell < 1 - 2 \times 10^{12}$ cm^{-2}), having the property that the net trapping rate increased when the electric field exceeded threshold. No such slow traps were found in unirradiated samples and none in gamma-irradiated devices. Since moderate energy proton damage is intermediate to that for gammas and fast neutrons, the introduction of slow traps with this type of field dependence may be diminished for protons relative to neutrons. Also observed in reference 6 were decreases in low-field mobility in Hall samples and in Gunn diodes, and the changes in $\bar{r}$ were attributed to changes in low-field mobility. For the proton experiment, arguments have been given for, at worst, only small changes in mobility relative to carrier density. On the other hand, large changes in $\bar{r}$ are observed (fig. 5).

Fast traps.- The changes in the low-frequency peak-to-valley current ratio as a function of proton fluence can be described on the basis of a fast trap model.

Fast traps are in equilibrium with the conduction band, for example, in equation (9) the net generation rate of carriers from the traps into the conduction band is large compared with $\partial J_e/\partial x$. Suppose that all of the radiation-produced traps are fast ($\bar{r} = r$) and that the efficiency is approximately given by

$$n = KC(\bar{n})\left(\frac{r - 1}{r + 1}\right) \tag{16}$$

Here $C(\bar{n})$ is the Copeland curve and K is a normalization factor dependent upon the voltage and current waveforms. Copeland's curve is not strictly valid for fast traps, and it is not clear what value of carrier density $\bar{n}$ to use for the best approximation of efficiency.

Examination of the data shows that the peak current as a function of proton fluence falls approximately on the plot of low-field carrier concentration. Thus, $I_p \propto n$, and by equation (2) $I_v \approx n'eAv_s$. This evaluation gives for the peak-to-valley current ratio

$$r \equiv \frac{I_p}{I_v} \approx \text{Const} \times \frac{n}{n'} \approx \text{Const} \times \left(\frac{1 - \frac{\alpha}{n_o}\Phi}{1 - \frac{\alpha'}{n_o}\Phi}\right) \tag{17}$$

According to the assumptions of this study, r and $\bar{r}$ decrease with fluence because the carrier removal rate for low fields is greater than that for high fields by roughly a factor of 2.

For purposes of illustration $\bar{n} = n'$ is chosen for substitution into $C(\bar{n})$. Figures 12 and 13 give comparisons of the calculated (from eq. (16)) and measured normalized efficiencies as functions of proton fluence for diodes D_3 and D_5 $\left(n_o \approx 4 \times 10^{15}\ \text{cm}^{-3}\right)$, respectively. In both cases, the calculated curves from equation (16) initially decrease with fluence and that of figure 12 has a subsequent relative maximum before decreasing again. The apparent value of equation (16) is that it does not predict initial increases for an initial carrier concentration $n_o \approx 4 \times 10^{15}\ \text{cm}^{-3}$. However, if n_o had been $\approx 2.5 \times 10^{15}\ \text{cm}^{-3}$ for D_5, the Copeland curves would have greater slopes in this region; and an initial increase would be expected by use of equation (16).

Intermediate traps.- It seems more probable that the radiation-produced traps comprise a mixture of the three types, perhaps favoring those with slow and intermediate response times. No approximate analytic form is available for efficiency in the presence of intermediate-response-time traps but the mechanism is expected to degrade efficiency and may account for the more rapid degradation than that predicted by equation (16). Other sources of difficulty are possible in the theoretical relations, for example, when long samples with fully developed domains are assumed. Such an assumption becomes questionable as the domain becomes large, or equivalently, when the operating dc field becomes large.

Noise

Two evident sources of FM noise are fluctuations in: (1) the time between domain annihilation and creation, and (2) the transit time of the high-field domain. Except for the anomalous behavior of one device, four out of five diodes produced no significant increase in FM noise in the band between 100 Hz and 50 kHz. Recall from a previous discussion the plausibility for assuming that the scattering-limited drift velocity and carrier mobility are relatively insensitive to the proton irradiations. Hence, the observation of small FM noise changes attributable to the transit time of the high-field domain is consistent with this assumption.

Increases in the noise power spectrum can be partly attributed to radiation-induced traps that have time constants on the order of the period of the microwave oscillation. These traps were referred to earlier as intermediate traps. Carrier capture and release from the traps are random events governed by transition probability rates. This result suggests the presence of a Fourier power spectrum in the vicinity of and overlapping the center frequency of oscillation.

CONCLUDING REMARKS

Direct-current measurements show that the conductance, peak current, valley current, and the high-field saturation current decrease with increasing proton irradiation levels. Although measurement of the carrier mobility of the Gunn devices was not possible, arguments are given to support the contention that changes in mobility are negligible relative to changes in carrier density for the proton-fluence levels attained in this experiment. It is established that scattering-limited velocities are attained and uniform carrier density exists in the active region of the n^+-n-n^+ structure for applied voltages high enough to assure that the microwave oscillations have vanished. From these considerations it is proposed that the electron carrier density decreases with increasing proton irradiation levels. Further, it is proposed that the carrier density at high fields is significantly greater than at low fields, and the difference increases with proton exposure.

Radio-frequency power measurements demonstrate that the diode efficiency decreases with fluence for devices having $n\ell \approx 2 \times 10^{12}$ cm^{-2} and $n\ell \approx 4 \times 10^{12}$ cm^{-2}. Carrier removal alone is not sufficient to explain the efficiency decrease for the samples having $n\ell \approx 4 \times 10^{12}$ cm^{-2}. Frequency-modulation noise was generally unaffected by radiation, but the magnitude of the noise in the noise power spectrum increased significantly. These effects are partially accounted for, in a qualitative fashion, by a model of radiation-produced electron traps having field-dependent net carrier capture rates and various response times.

Langley Research Center,
National Aeronautics and Space Administration,
Hampton, Va., October 1, 1973.

REFERENCES

1. Wysocki, Joseph J.: Radiation Studies on GaAs and Si Devices. IEEE Trans. Nucl. Sci., vol. NS-10, no. 5, Nov. 1963, pp. 60-65.

2. Aukerman, L. W.; Davis, P. W.; Graft, R. D.; and Shilliday, T. S.: Radiation Effects in GaAs. J. Appl. Phys., vol. 34, no. 12, Dec. 1963, pp. 3590-3599.

3. Stein, H. J.: Electrical Studies of Low-Temperature Neutron- and Electron-Irradiated Epitaxial n-Type GaAs. J. Appl. Phys., vol. 40, no. 13, Dec. 1969, pp. 5300-5307.

4. Marcus, G. H.; and Bruemmer, H. P.: Radiation Damage in GaAs Gunn Diodes. IEEE Trans. Nucl. Sci., vol. NS-17, no. 6, Dec. 1970, pp. 230-232.

5. McNichols, J. L.; and Ginell, W. S.: Predicted Effects of Neutron Irradiation on GaAs Junction Field Effect Transistors. IEEE Trans. Nucl. Sci., vol. NS-17, no. 2, Apr. 1970, pp. 52-54.

6. Berg, N.; and Dropkin, H.: Neutron Displacement Effects in Epitaxial Gunn Diodes. IEEE Trans. Nucl. Sci., vol. NS-17, no. 6, Dec. 1970, pp. 233-238.

7. Brehm, Gailon E.; and Pearson, Gerald L.: Effects of Gamma Radiation on Gunn Diodes. IEEE Trans. Electron Devices, vol. ED-17, no. 6, June 1970, pp. 475-479.

8. Josenhans, J.: Noise Spectra of Read Diode and Gunn Oscillators. Proc. IEEE, vol. 54, no. 10, Oct. 1966, pp. 1478-1479.

9. Crawford, J. H., Jr.: Radiation Effects in Diamond Lattice Semiconductors. IEEE Trans. Nucl. Sci., vol. NS-10, no. 5, Nov. 1963, pp. 1-10.

10. Copeland, John A.: Theoretical Study of a Gunn Diode in a Resonant Circuit. IEEE Trans. Electron Devices, vol. ED-14, no. 2, Feb. 1967, pp. 55-58.

11. Kino, Gordon S.; and Kuru, Isam: High-Efficiency Operation of a Gunn Oscillator in the Domain Mode. IEEE Trans. Electron Devices, vol. ED-16, no. 9, Sept. 1969, pp. 735-748.

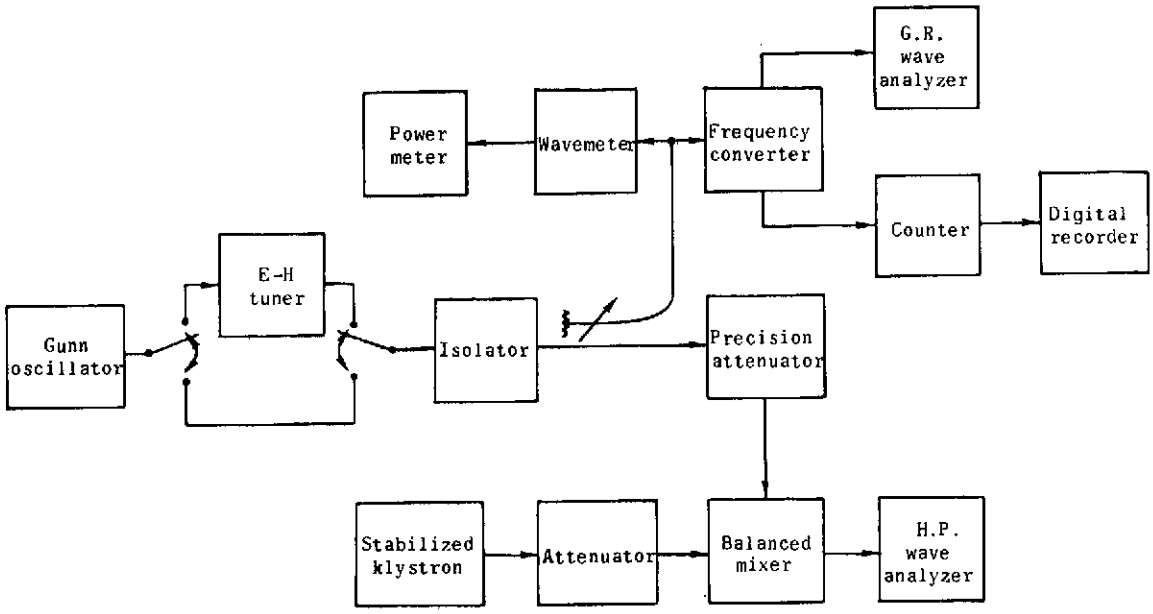

Figure 1.- Radio-frequency measurement system.

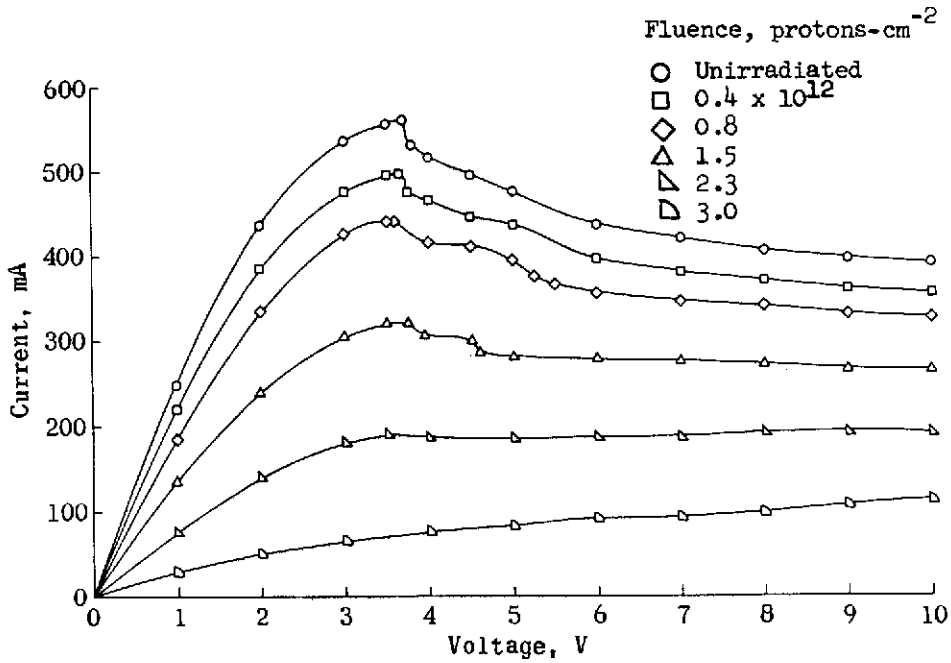

Figure 2.- Typical current-voltage curves for various proton fluences.

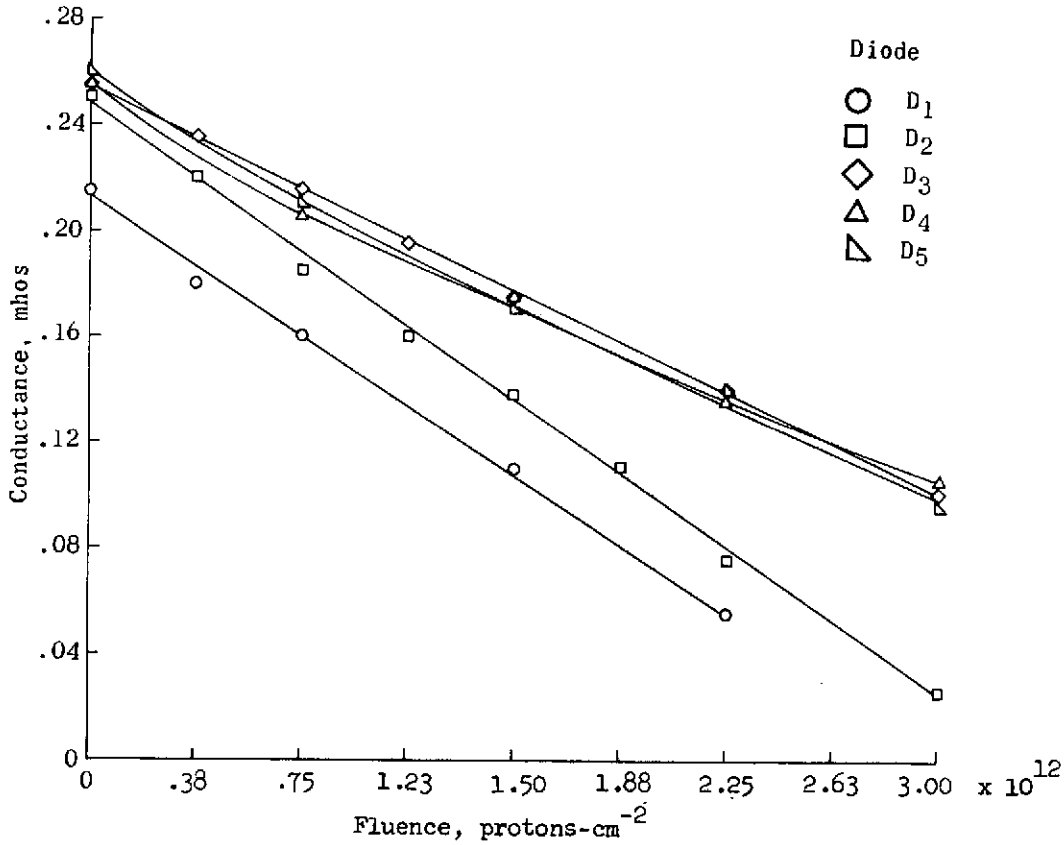

Figure 3.- Variation of low-field conductance with proton fluence for diodes D_1 to D_5.

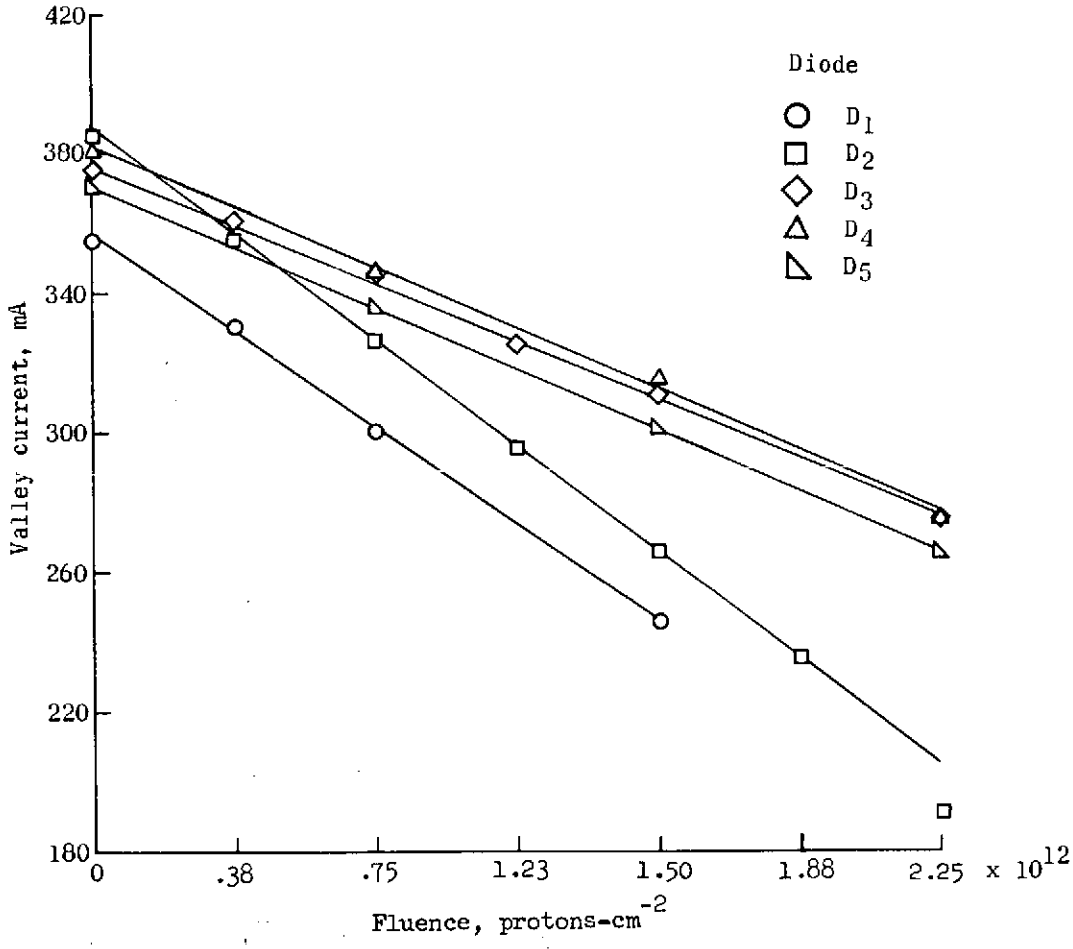

Figure 4.- Variation of valley (saturation) current with proton fluence for diodes D_1 to D_5.

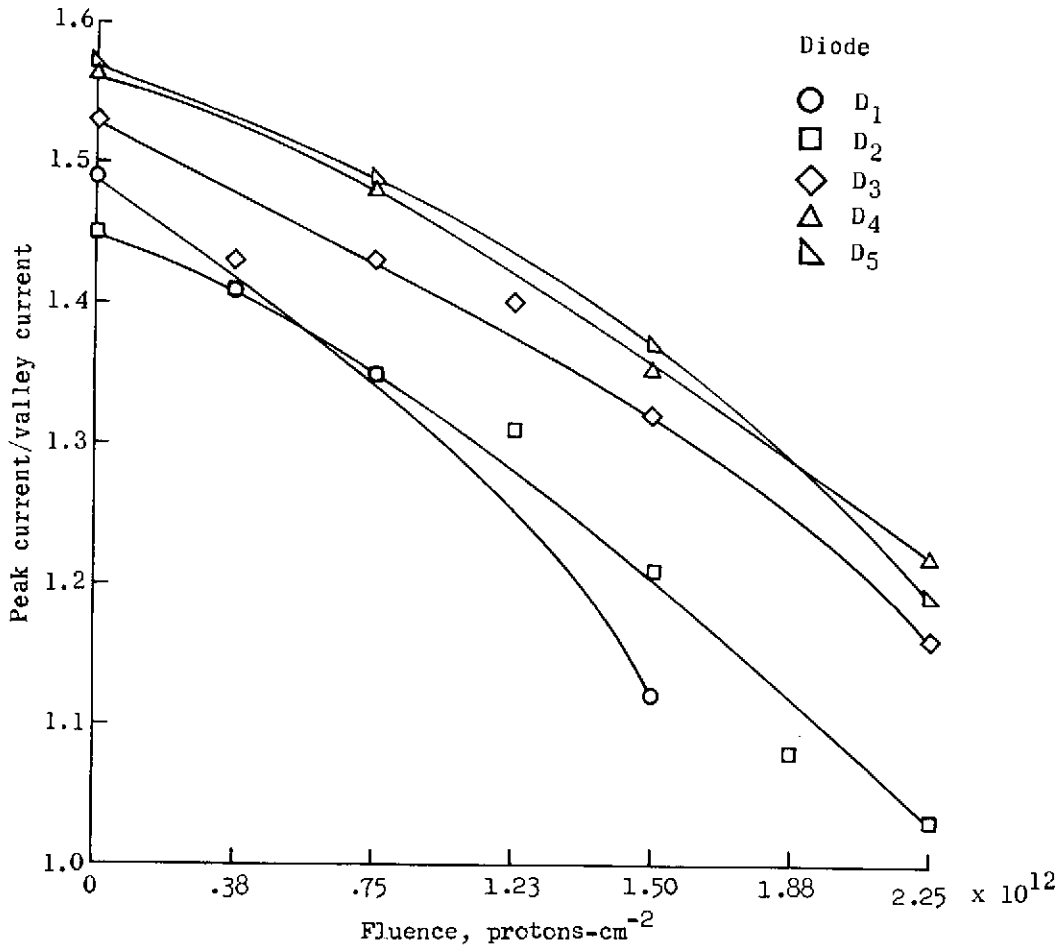

Figure 5.- Variation of peak-to-valley current ratio with proton fluence for diodes D_1 to D_5.

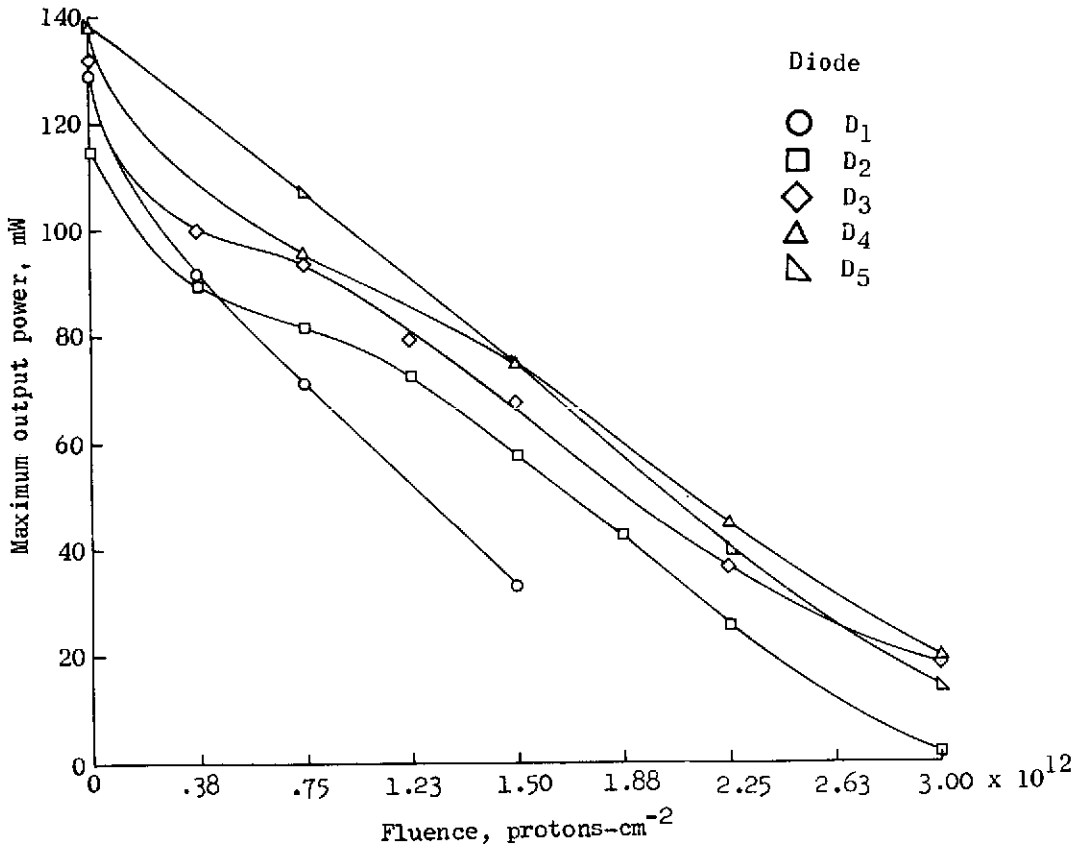

Figure 6.- Maximum output power as a function of proton fluence for diodes D_1 to D_5.

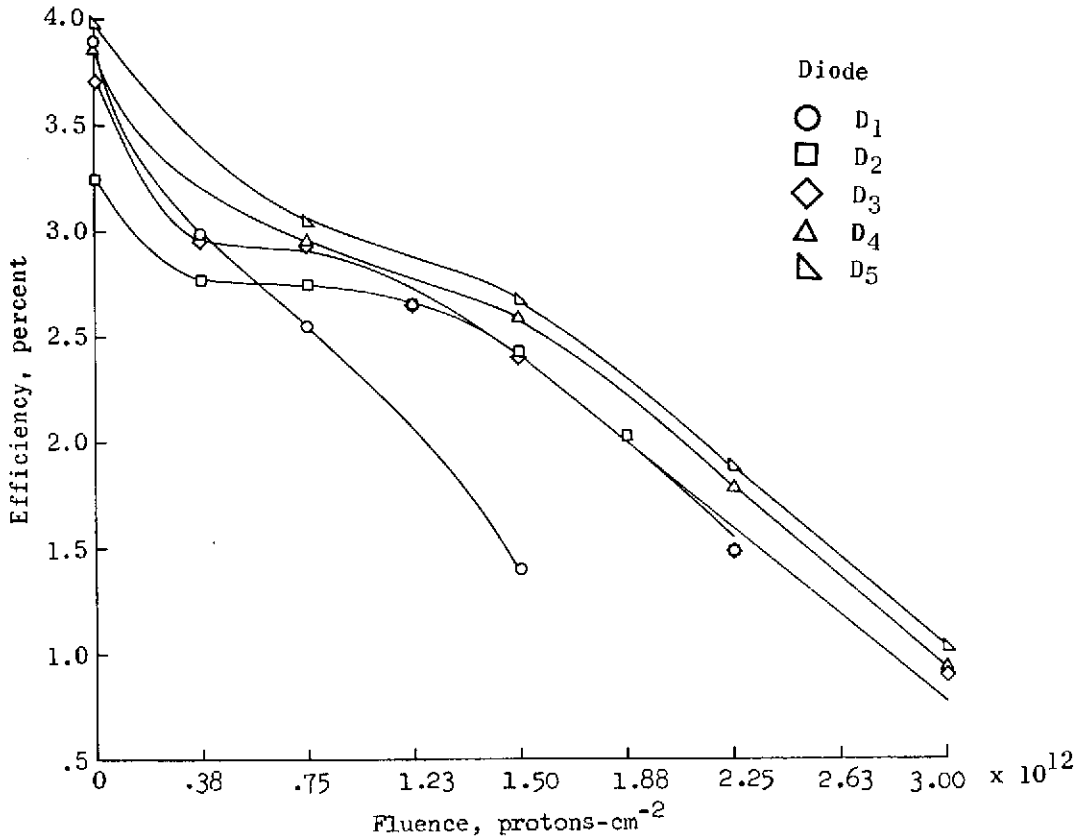

Figure 7.- Efficiency as a function of proton fluence for diodes D_1 to D_5.

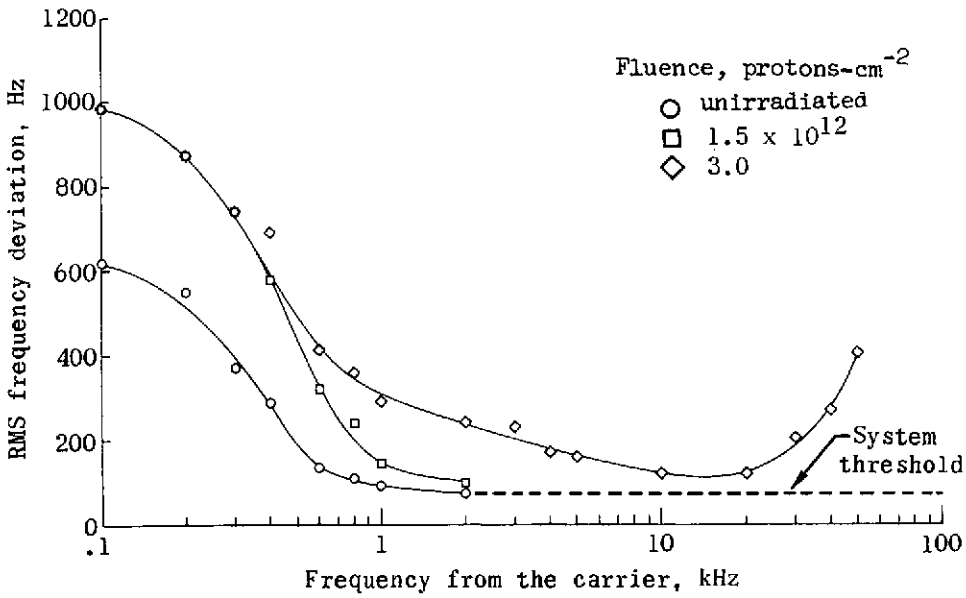

Figure 8.- Frequency-modulation noise spectrum as a function of proton fluence for diode D_4.

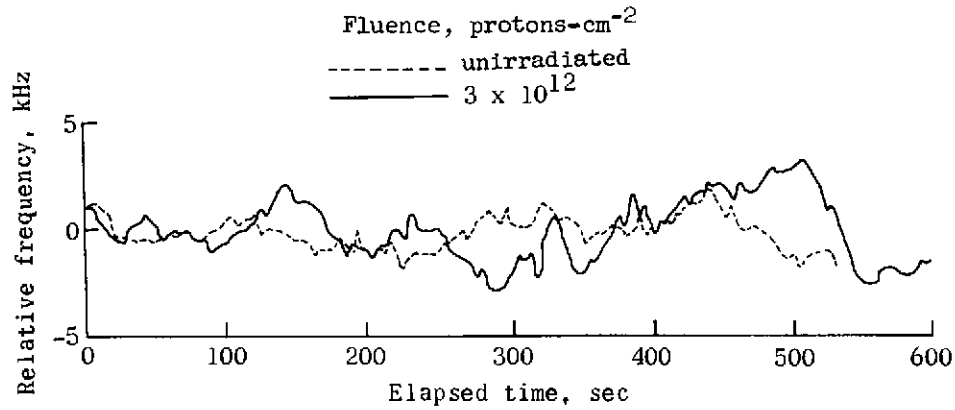

Figure 9.- Frequency drift as a function of proton fluence for diode D_1.

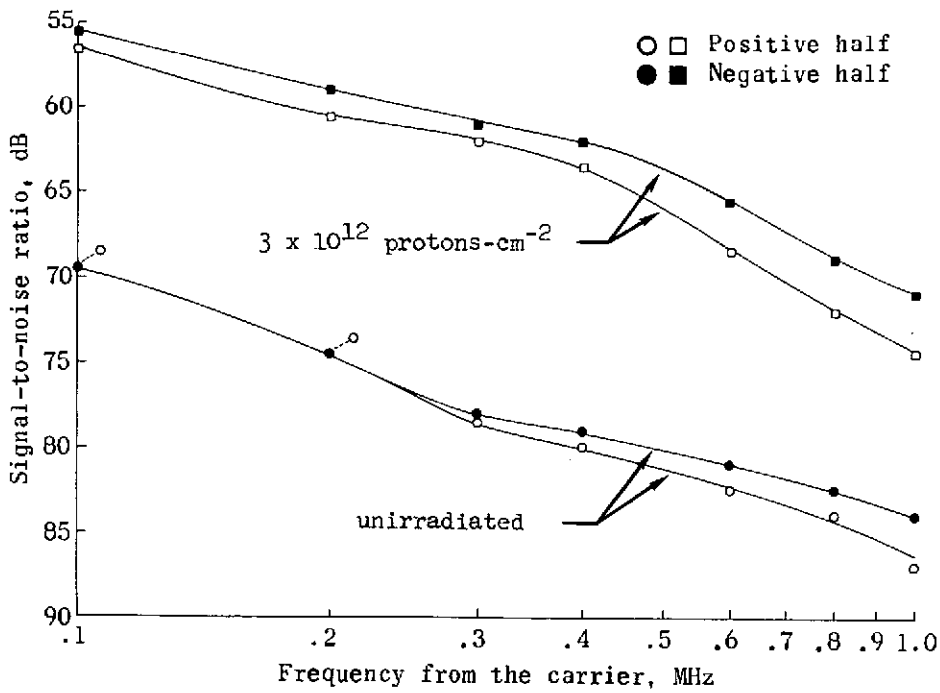

Figure 10.- Noise power spectrum as affected by proton fluence for diode D_3.

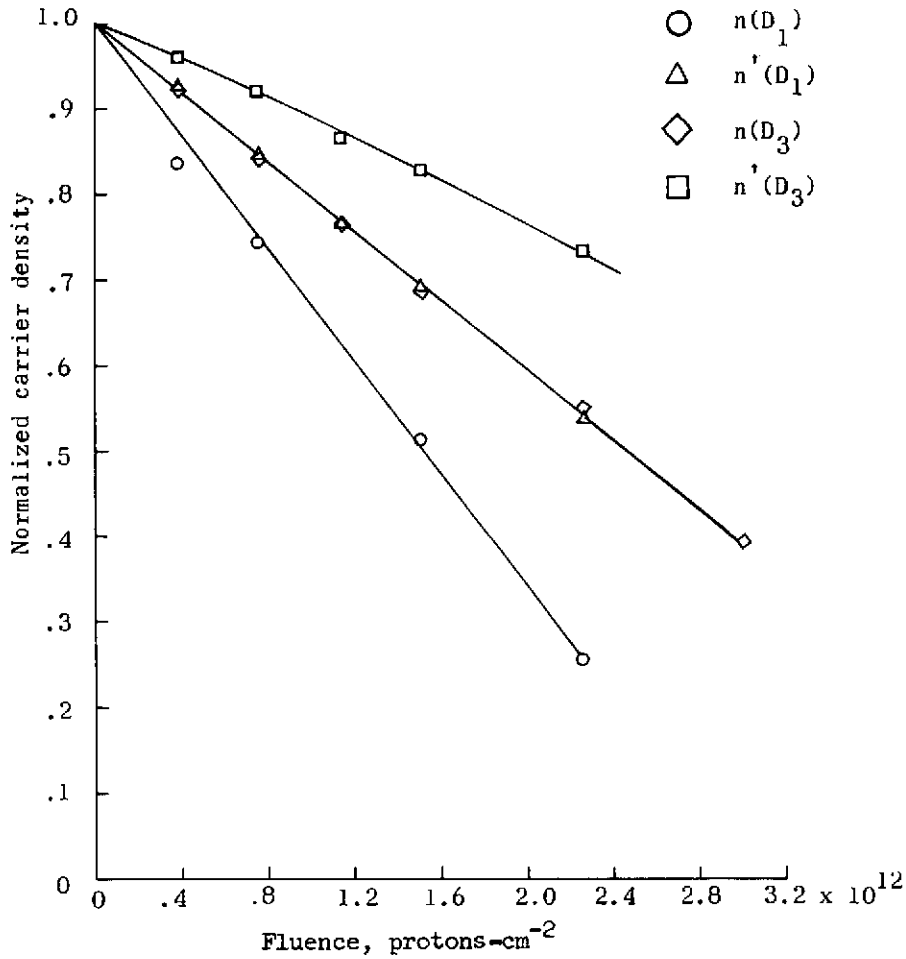

Figure 11.- Normalized carrier density, low field (n) and high field (n'), for diodes D_1 and D_3.

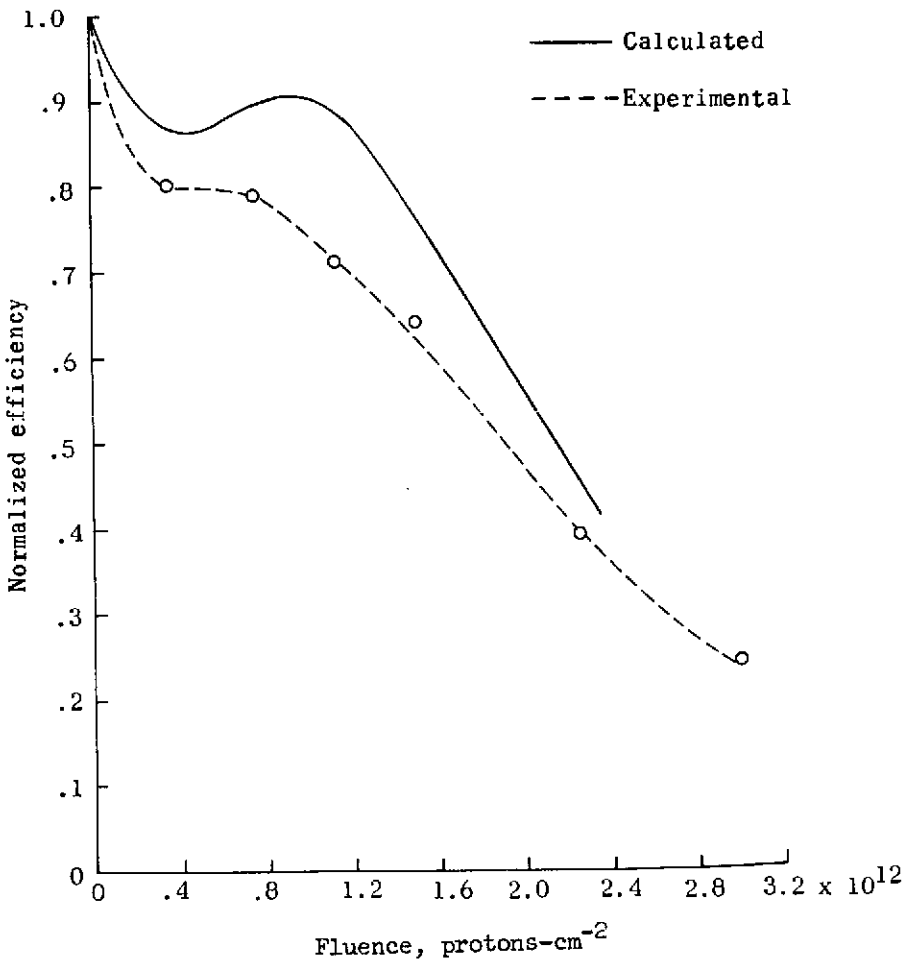

Figure 12.- Calculated and experimental normalized efficiency as a function of proton fluence for diode D_3.

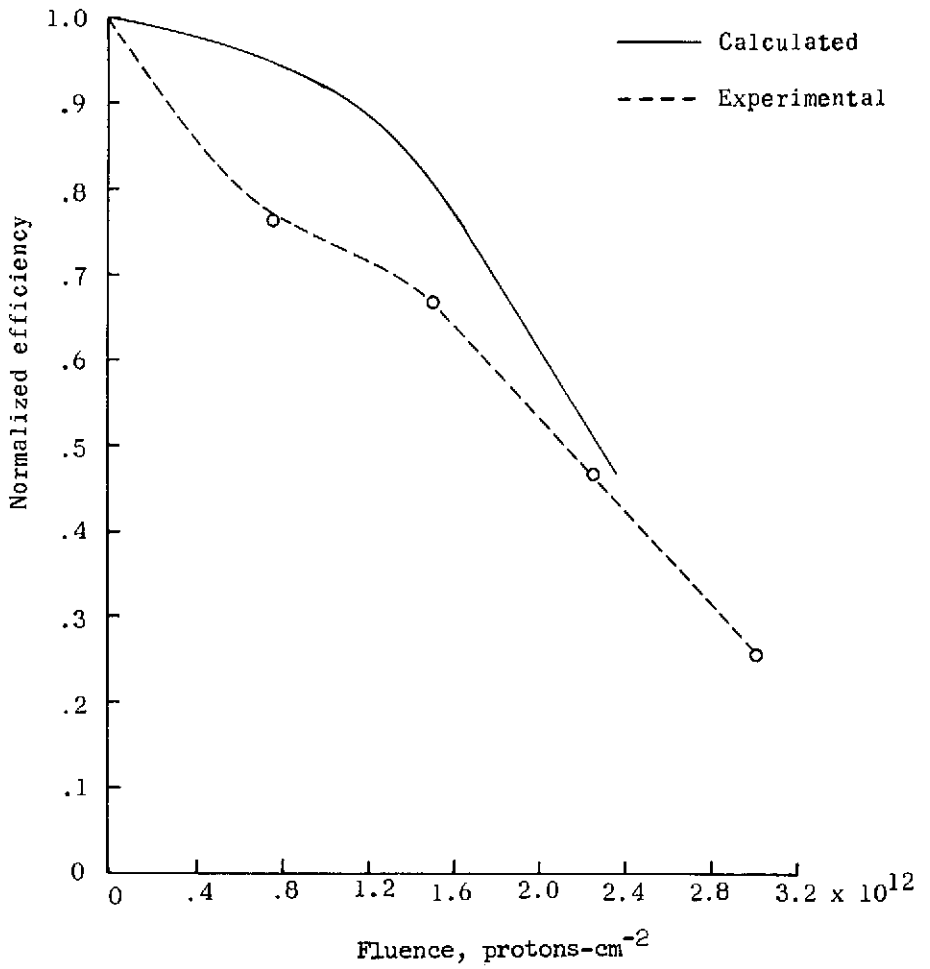

Figure 13.- Calculated and experimental normalized efficiency as a function of proton fluence for diode D_5.